

Comprehensive Analysis Identified the Circadian Clock and Global Circadian Gene Expression in Human Corneal Endothelial Cells

Hiroko Nakai,^{1,2} Yoshiki Tsuchiya,¹ Nobuya Koike,¹ Taiki Asano,¹ Morio Ueno,² Yasuhiro Umemura,¹ Yuh Sasawaki,¹ Ryutaro Ono,¹ Junji Hamuro,² Chie Sotozono,² and Kazuhiro Yagita¹

¹Department of Physiology and Systems Bioscience, Kyoto Prefectural University of Medicine, Kyoto, Japan

²Department of Ophthalmology, Kyoto Prefectural University of Medicine, Kyoto, Japan

Correspondence: Yoshiki Tsuchiya, Department of Physiology and Systems Bioscience, Kyoto Prefectural University of Medicine, Kawaramachi-Hirokoji, Kyoto 602-8566, Japan;

ytsuchi@koto.kpu-m.ac.jp

Kazuhiro Yagita, Department of Physiology and Systems Bioscience, Kyoto Prefectural University of Medicine, Kawaramachi-Hirokoji, Kyoto 602-8566, Japan;

kyagita@koto.kpu-m.ac.jp

HN and YT contributed equally to the work presented here and should therefore be regarded as equivalent authors.

Received: January 11, 2022

Accepted: April 25, 2022

Published: May 17, 2022

Citation: Nakai H, Tsuchiya Y, Koike N, et al. Comprehensive analysis identified the circadian clock and global circadian gene expression in human corneal endothelial cells.

Invest Ophthalmol Vis

Sci. 2022;63(5):16.

<https://doi.org/10.1167/iovs.63.5.16>

PURPOSE. To investigate circadian clock oscillation and circadian global gene expression in cultured human corneal endothelial cells (cHCECs) to elucidate and assess the potential function of circadian regulation in HCECs.

METHODS. In this study, we introduced a circadian bioluminescence reporter, *Bmal1:luciferase* (*Bmal1:luc*), into cHCECs and subsequently monitored real-time bioluminescence rhythms. RNA-sequencing data analysis was then performed using sequential time-course samples of the cHCECs to obtain a comprehensive understanding of the circadian gene expression rhythms. The potential relevance of rhythmically expressed genes was then assessed by systematic approaches using functional clustering and individual gene annotations.

RESULTS. *Bmal1:luc* bioluminescence exhibited clear circadian oscillation in the cHCECs. The core clock genes and clock-related genes showed high-amplitude robust circadian messenger RNA (mRNA) expression rhythms in cHCECs after treatment with dexamethasone, and 329 genes that exhibited circadian mRNA expression rhythms were identified (i.e., genes involved in various physiological processes including glycolysis, mitochondrial function, antioxidative systems, hypoxic responses, apoptosis, and extracellular matrix regulation, which represent the physiological functions of HCECs).

CONCLUSIONS. Our findings revealed that cHCECs have a robust and functional circadian clock, and our discovery that a large number of genes exhibit circadian mRNA expression rhythms in cHCECs suggests a potential contribution of circadian regulation to fine-tune HCEC functions for daily changes in the environment.

Keywords: corneal endothelial cells, circadian rhythm, gene expression

The circadian clock is a fundamental system in most organisms living on Earth, as it regulates diverse behavioral and physiological functions. In mammals, the master circadian pacemaker resides in the suprachiasmatic nucleus of the hypothalamus and coordinates other peripheral circadian oscillators distributed throughout the body, including the eyes.¹⁻⁶ In all mammalian cells, a set of transcription factors comprised of cell-autonomous transcriptional and translational feedback loops lead to circadian rhythms of gene expression. The transcription factors CLOCK and BMAL1 heterodimerize and positively regulate transcription of *Period* (*PER1*, *PER2*, and *PER3*) and *Cryptochrome* (*CRY1* and *CRY2*) genes. The produced PER and CRY proteins repress transcriptional activity of CLOCK/BMAL1 heterodimers and downregulate their own transcription, thus constituting the primary feedback loop.^{7,8} The expres-

sion of *BMAL1* is also controlled by a secondary feedback loop in which retinoic acid receptor-related orphan receptor (*ROR*) α and *ROR* γ transactivate and *REV-ERB* α and *REV-ERB* β repress *BMAL1* expression by competing bindings at the *BMAL1* promoter.^{9,10} These transcriptional loops regulate circadian expression of diverse clock-controlled output genes.

In the eye, the circadian clock may contribute to diurnal fluctuations in the physiological functions, such as intraocular pressure, anterior chamber depth, choroidal thickness, and ocular length.^{11,12} These diurnal variations are thought to be important for normal physiology of the eye and are related to ocular diseases such as glaucoma, myopia, and central serous chorioretinopathy. Moreover, previous studies have revealed diurnal variation in both corneal curvature and thickness.¹³⁻¹⁷ Because the cornea is exposed to diurnal

environmental changes, such as daytime light and nighttime hypoxic conditions due to long periods of eyelid closure during sleep, corneal cells might possibly have the ability to predict and adapt to these environmental changes. During morning hours, patients afflicted with bullous keratopathy typically often experience worse vision. The findings in a study on diurnal variation of corneal edema in Fuchs endothelial corneal dystrophy (FECD) demonstrated that a noticeable degree of morning edema exists in corneas with advanced FECD, yet it resolves within the first 4 hours after the eye is first opened.¹⁸ For decades, clinicians have explained that morning corneal edema is due to decreased oxygen levels beneath the closed eyelid during sleep.^{19–21} However, the specific mechanism has yet to be fully elucidated.

It has been reported that in mice, circadian expression of PER2::LUCIFERASE (PER2::LUC) bioluminescence reporter is observed in both the corneal epithelial and endothelial layers.²² In a previous rabbit-model study on corneal epithelial cells, the findings revealed circadian rhythms in the regeneration of the corneal epithelium.²³ Although corneal endothelial cells (CECs) also play pivotal roles in the maintenance of corneal functions and homeostasis, the circadian regulation of CECs has yet to be well described.

In this present study, we investigated intracellular circadian clock function in cultured human CECs (cHCECs) by using mature differentiated cells that mimic the characteristics of HCECs in healthy tissue *in vivo*.²⁴ We performed global expression analysis in HCECs to highlight the possible circadian regulation on human corneal endothelial functions as an important system allowing eyes to adapt to daily environmental changes.

MATERIALS AND METHODS

Donor Human Corneal Tissue and CECs

The human tissue used in this study was handled in accordance with the tenets of the Declaration of Helsinki. The HCECs used in the study were derived from donor corneas obtained from CorneaGen Inc. (Seattle, WA, USA) and were cultured prior to the experiments, with subsequent analysis being performed. Informed written consent for eye donation for research was obtained from the next of kin of all deceased donors. All tissues were recovered under the tenets of the Uniform Anatomical Gift Act of the particular state in which the donor consent was obtained and the tissue was recovered. All donor corneas were preserved in Optisol-GS (Chiron Vision, Irvine, CA, USA) corneal storage medium and then shipped via international air transport for research purposes. Donor information accompanying the donor corneas showed that all donors were considered healthy and absent of any corneal disease at the time when the corneas were obtained.

Cultured HCECs

The HCECs were cultured according to the previously published protocols, but with some modifications.^{25–29} Briefly, Descemet's membranes with CECs were stripped from the donor corneas and digested at 37°C with 1 mg/mL collagenase A (Roche Applied Science, Penzberg, Germany) for 2 hours. The HCECs obtained from a single donor cornea were then seeded in one well of a type I collagen-coated six-well plate (Corning, Inc., Corning, NY, USA). The culture

medium was prepared according to the published protocols.^{25–29} The HCECs were then passaged after harvest with 10× TrypLE Select (Thermo Fisher Scientific, Waltham, MA, USA) treatment at 37°C for 12 minutes after reaching confluence. The HCECs at passages two to four were used for all experiments. Phase-contrast images of the HCECs were obtained via the use of an inverted microscope system (CKX41; Olympus Corporation, Tokyo, Japan).

Flow Cytometry Analysis of cHCECs

The HCECs were collected from the culture dish by TrypLE Select treatment and suspended at a concentration of 4×10^6 cells/mL in fluorescence-activated cell sorting (FACS) buffer (i.e., phosphate buffered saline containing 1% bovine serum albumin and 0.05% NaN₃). Next, an equal volume of antibody solution was added and incubated at 4°C for 2 hours. The antibodies used were as follows: fluorescein isothiocyanate-conjugated anti-human CD90 monoclonal antibody (mAb), phycoerythrin (PE)-conjugated anti-human CD166 mAb, PerCP-Cy5.5 conjugated anti-human CD24 mAb, and PE/Cy7-conjugated anti-human CD44 (all obtained from BD Biosciences, San Jose, CA, USA), as well as eBioscience allophycocyanin (APC)-conjugated anti-human CD105 (Thermo Fisher Scientific). After washing with FACS buffer, the HCECs were analyzed by use of the BD FACSCanto II Flow Cytometry System (BD Biosciences).

Reagents

Rho-associated protein kinase inhibitor Y-27632 was obtained from Wako Pure Chemical Industries, Ltd. (Osaka, Japan). Fetal bovine serum was obtained from Thermo Fisher Scientific, and plastic culture plates were obtained from Corning.

Plasmids and Transfection

At 1 day after passage, the cells were transfected with the *Bmal1:luciferase* (*Bmal1:luc*)–pT2A plasmid³⁰ and the Tol2 transposase expression vector pCAGGS-TP by using FuGENE HD Transfection Reagent (Promega Corporation, Madison, WI, USA) according to the manufacturer's instructions.

Bioluminescence Imaging

For bioluminescence imaging, the medium was replaced with a medium containing 0.2-mM luciferin with or without 100-nM dexamethasone (DEX). Next, via the use of a bioluminescence microscope imaging system (LV200 LUMINOVIEW; Olympus Corporation), 20-minute-exposure time-lapse images of the cells were collected at 60-minute intervals.

Period Analysis

The data recorded via use of the LV200 LUMINOVIEW bioluminescence microscope image system were analyzed using a sine-wave fitting. A linear baseline was subtracted from the raw data, and each value was then further divided by the standard deviation within the sliding 24-hour window for amplitude normalization. The detrended data from 13 to

72 hours were then used for analysis. The sine-wave fitting was performed using the following equation:

$$y(t) = A \sin\left(\frac{2\pi(t - \varphi)}{\tau}\right)$$

where A = amplitude, t = time, τ = period, and φ = phase.

RNA Sequencing

We used cHCECs cultured from a single donor cornea. The medium of cHCECs was replaced with a medium containing 100-nM DEX, which was present throughout the time-course experiment. The cells were frozen at the indicated time points. Cells were harvested from a dish per one time point over two complete circadian cycles. Total RNA was extracted from the cells via use of the miRNeasy Kit (QIAGEN, Hilden, Germany) according to the manufacturer's instructions. PolyA RNA selection, library construction using the TruSeq RNA Sample Prep Kit v2 (Illumina, Inc., San Diego, CA, USA), and RNA sequencing (RNA-seq) was performed by Macrogen Japan (Tokyo, Japan) using the NovaSeq 6000 Sequencing System (Illumina) with 101-bp paired-end reads according to the manufacturer's instructions. After adaptor sequence trimming using the Java application Trimmomatic was performed,³¹ the sequenced reads were mapped to the human genome (GRCh38/hg38) using the STAR open-source software package.³² To obtain reliable alignments, the reads with a mapping quality of less than 10 were removed by the SAMtools set of utilities.³³ The known canonical gene set (60,675 genes) in the University of California, Santa Cruz, GENCODE Gene Track Version 36 was used for annotation, and the reads mapped to the exons were quantified using the HOMER analysis suite³⁴ as previously described.³⁵ To report one isoform per locus (gene symbol), the highest expressed isoform was chosen. A gene was assumed to be expressed if there were more than 20 reads mapped, on average, in the exon of the gene. An expression level cutoff—average fragments per kilobase of exon per million reads (FPKMs) of > 0.5 —was used for the downstream data analysis. RNA cycling was determined using Metacycle (an integrated R package to evaluate periodicity in large-scale data; R Foundation for Statistical Computing, Vienna, Austria)³⁶ with $P < 0.05$, rAMP of > 0.1 , and the following options: minper = 20, maxper = 28, cycMethod = c("ARS","JTK","LS"), analysisStrategy = "auto," outputFile = TRUE, outIntegration = "both," adjustPhase = "predictedPer," combinePvalue = "fisher," weightedPerPha = TRUE, ARSmle = "auto," and ARSdefaultPer = 24. The functional enrichment analysis on the identified gene list was performed via the use of Metascape.³⁷ To compare the global gene expression profile obtained from the cHCEC samples with that in the previous study.³⁸ Sequence Read Archive (SRA) files in GSE65991 were downloaded from the SRA (National Center for Biotechnology Information, Bethesda, MD, USA), converted to FASTQ files using the National Center for Biotechnology Information SRA Toolkit, and then analyzed as described above. A Chow–Ruskey diagram of the multiple comparison overlaps of the expressed genes was made with R using the Vennerable package.³⁹ DESeq2 rlog-transformed raw counts of genes expressed in at least one cell type in the Chow–Ruskey diagram (17,557) were used for hierarchical cluster analysis using hclust from the standard R package.

Real-Time Quantitative PCR

Total RNA was subjected to cDNA synthesis with random hexamer primers and M-MLV Reverse Transcriptase (Thermo Fisher Scientific), a recombinant DNA polymerase, according to the manufacturer's instructions. Real-time quantitative polymerase chain reaction (qPCR) was performed via the use of iTaq Universal SYBR Green Supermix (Bio-Rad Laboratories, Inc., Hercules, CA, USA) and the StepOne-Plus Real-Time PCR System (Thermo Fisher Scientific). The primer sequences used for qPCR are listed in Supplementary Table S1.

RESULTS

Robust Circadian Rhythms of *Bmal1:luc* Reporter Expression in cHCECs

To assess the circadian clock function in HCECs, we introduced a circadian bioluminescence reporter, *Bmal1:luc*, in which transcription of the luciferase gene is driven by promoter of a core clock gene, *Bmal1*, into cHCECs derived from an adult donor (Fig. 1A). After repeated passaging of the cHCECs, *Bmal1:luc* bioluminescence was recorded via the use of a high-sensitivity, electron-multiplying, charge-coupled-device camera-based microscope. A bioluminescence image displaying cells with the *Bmal1:luc* reporter is shown in Figure 1B. Sequential imaging clearly demonstrated time-dependent fluctuations of bioluminescence (Fig. 1C; Supplementary Video). Quantification of the bioluminescence revealed that most cells showed clear circadian oscillation of *Bmal1:luc* bioluminescence (Fig. 1D). Periods of bioluminescence rhythms were calculated from single-cell recordings distributed in the range of 20.2 to 25.4 hours, and the mean period was 22.5 hours (Fig. 1E). Our findings clearly indicate that the cHCECs have the functional circadian clock machinery of transcriptional/translational feedback loops.

To assess the susceptibility of the circadian clock in the cHCECs to resetting by an external stimulus, the cells were treated with a medium containing DEX that is known to entrain the peripheral circadian clock. Our findings showed that the amplitude of bioluminescence rhythms in a cell population was increased upon DEX treatment of the cells (Fig. 1F). Taken together, these findings suggest that cHCECs possess cell-autonomous and entrainable circadian oscillators.

Global Gene Expression Analysis of cHCECs

To understand the circadian gene expression network and its possible physiological impact on the local circadian clockwork in cHCECs, the cells were entrained with DEX and total RNA was extracted from the cells at 4-hour intervals over a 2-day period (range, 16–64 hours) after DEX treatment. RNA samples from the cHCECs were then analyzed by polyA RNA selection and RNA-seq. We first compared the global gene expression profile obtained from our cHCEC samples with that obtained in the previous study, which provides transcriptome analyses of ex vivo HCEC culture (evHCEnC) and primary HCEC culture (pHCEnC), and distinct HCEC lines (HCEnC and HCEC).³⁸ Our findings revealed that 10,562 out of 13,499 genes (i.e., more than 78% of expressed genes) were overlapped among the HCEC samples (Fig. 2A; Supplementary Table S2). Hierarchical clustering of HCEC

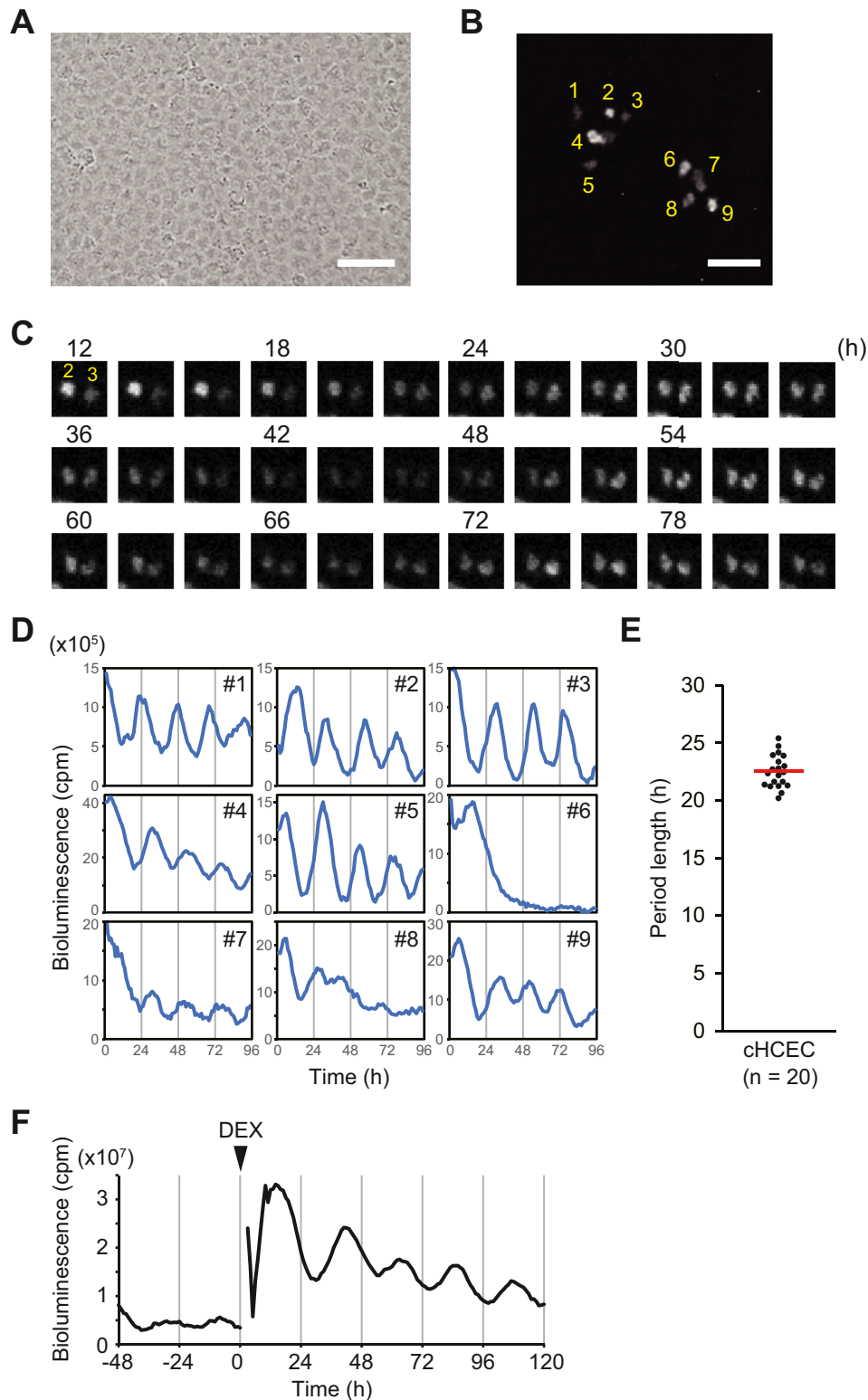


FIGURE 1. Circadian bioluminescence rhythms of the *Bmal1:luc* reporter in cHCECs. **(A)** A phase image of the cHCECs. *Scale bar:* 50 μm . **(B)** Representative bioluminescence image showing cells with *Bmal1:luc* reporter expression. Numbers indicate cells corresponding to the numbers in **(D)**. *Scale bar:* 100 μm . **(C)** Sequential bioluminescence images of cells #2 and #3 at 1-hour intervals. **(D)** Bioluminescence from each cell quantified and plotted on a graph. **(E)** The period of each bioluminescence rhythm was calculated and plotted (*black dots*). The *red line* indicates the mean period. **(F)** Circadian bioluminescence rhythms were entrained upon the exchange to the medium containing dexamethasone. Bioluminescence in a cell population was plotted. Time 0 indicates the timing of the medium exchange.

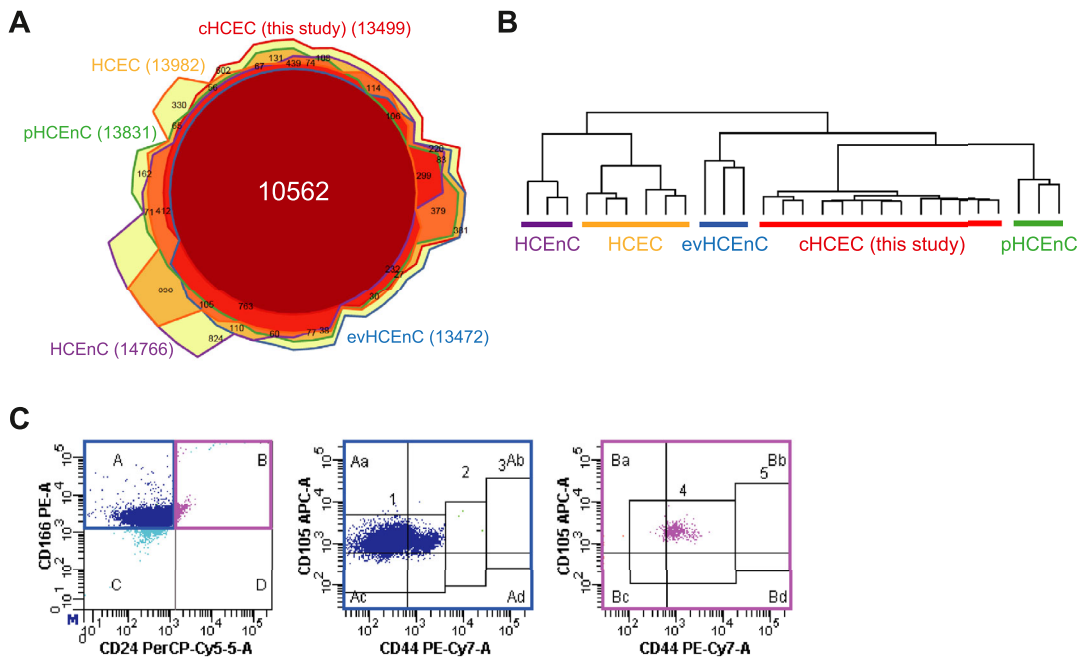


FIGURE 2. Global expression analysis validating the characteristics of cHCECs. (A) Chow–Ruskey diagram showing overlaps among expressed genes in our cHCECs and other HCECs reported in a previous study³⁸ (further described in the text). Each number in parentheses indicates the number of expressed genes in each cell type. Of all cell types analyzed, a total of 10,562 genes were found to be commonly expressed. (B) Hierarchical cluster analysis of gene expression profiles of 13 time-course samples of cHCECs with previously reported HCECs using the complete linkage method with Euclidean distance. (C) Flow cytometry analysis showing that the dominant population of cHCECs shows characteristics of in vivo healthy-tissue HCECs.

gene expression datasets further revealed that our cHCEC samples showed a close relationship with the evHCEC and pHCEC samples in the previous study, thus suggesting a gene expression profile similar to that of in vivo CECs (Fig. 2B); that is, the cHCECs are divided into subpopulations in which CD44⁻/dull mature differentiated cells without cell-state transition (CST) are selectively applicable for cell-based therapy.^{25,26,40} Flow cytometry analysis revealed that the majority of cHCECs showed CD166⁺/CD24⁻/CD26⁻/CD44⁻/dull/CD105⁻/dull characteristics that mimic the cell surface markers of in vivo healthy-tissue HCECs (Fig. 2C).²⁵ Collectively, these findings suggest that our cHCECs had the characteristics of in vivo HCECs.

Comprehensive Analysis of the Circadian Profiles of Global Gene Expression Rhythms in the cHCECs

Given the consistency and the validity of the gene expression profiles of the cHCECs, we next set out to explore potential circadian regulation of the global gene expression patterns. RNA-seq analysis revealed that as many as 329 genes were cyclically expressed within the standard range of a circadian period (Fig. 3A; Supplementary Table S3). The peak phase of mRNA expression of each gene varied throughout the circadian time (Fig. 3B). Of important interest, the core clock genes including *PER1*, *PER2*, *CRY1*, *CRY2*, and *BMAL1* (also called *ARNTL*) showed clear circadian oscillation of mRNA expression (Fig. 3C; Supplementary Fig. S1). *NR1D1* and *NR1D2*, which encode REV-ERB α and REV-ERB β , respectively, and *DBP*, which encodes a clock-related transcription factor, also exhibited circadian mRNA expression with high amplitudes. Phase analysis of clock and clock-related genes

demonstrated an obvious antiphase relationship between E-box-driven *PER1* and *PER2* and ROR-response-element-driven *BMAL1* and *NPAS2* (Fig. 3D). These results clearly indicate that the functional circadian transcriptional feedback loops are maintained in cHCECs with an adequate phase relationship.

Gene ontology analysis of the 329 cycling genes demonstrated that circadian rhythm was ranked at the top of the enriched terms (Fig. 3E). There are also other enriched terms related to several metabolic processes and signaling pathways. In the context of diurnal fluctuation of the availability of oxygen in the cornea, we first focused on genes involved in glycolysis, mitochondrial functions, and energy homeostasis and then identified a set of oscillating genes, including *PDK4*, *SLC25A10*, *MTHFD1L*, *LDHD*, *MTERF2*, *MAP1LC3C*, *PRKAG2*, *DEPTOR*, *AKR1C1*, *AKR1C3*, *ALFH3A2*, and *ALDH4A1* (Fig. 3F; also see Discussion). These findings suggest the possibility that glycolysis and mitochondrial functions can be affected by the intrinsic circadian clock in CECs.

Implication of Circadian Gene Expression for Human Corneal Physiology

To further identify rhythmically expressed genes with potential relevance in the physiology of CECs, we surveyed the gene clusters involved in corneal endothelial functions by using a list of the top 100 abundantly expressed genes. Our findings revealed a number of genes that were previously identified as highly expressed genes in HCECs^{41–43} and that those abundantly expressed genes are related to ion transport (*ATP1A1*, *SLC4A11*, *CA2*, *CA3*, *CA12*, and *AQP1*), extracellular matrix (ECM) regulation

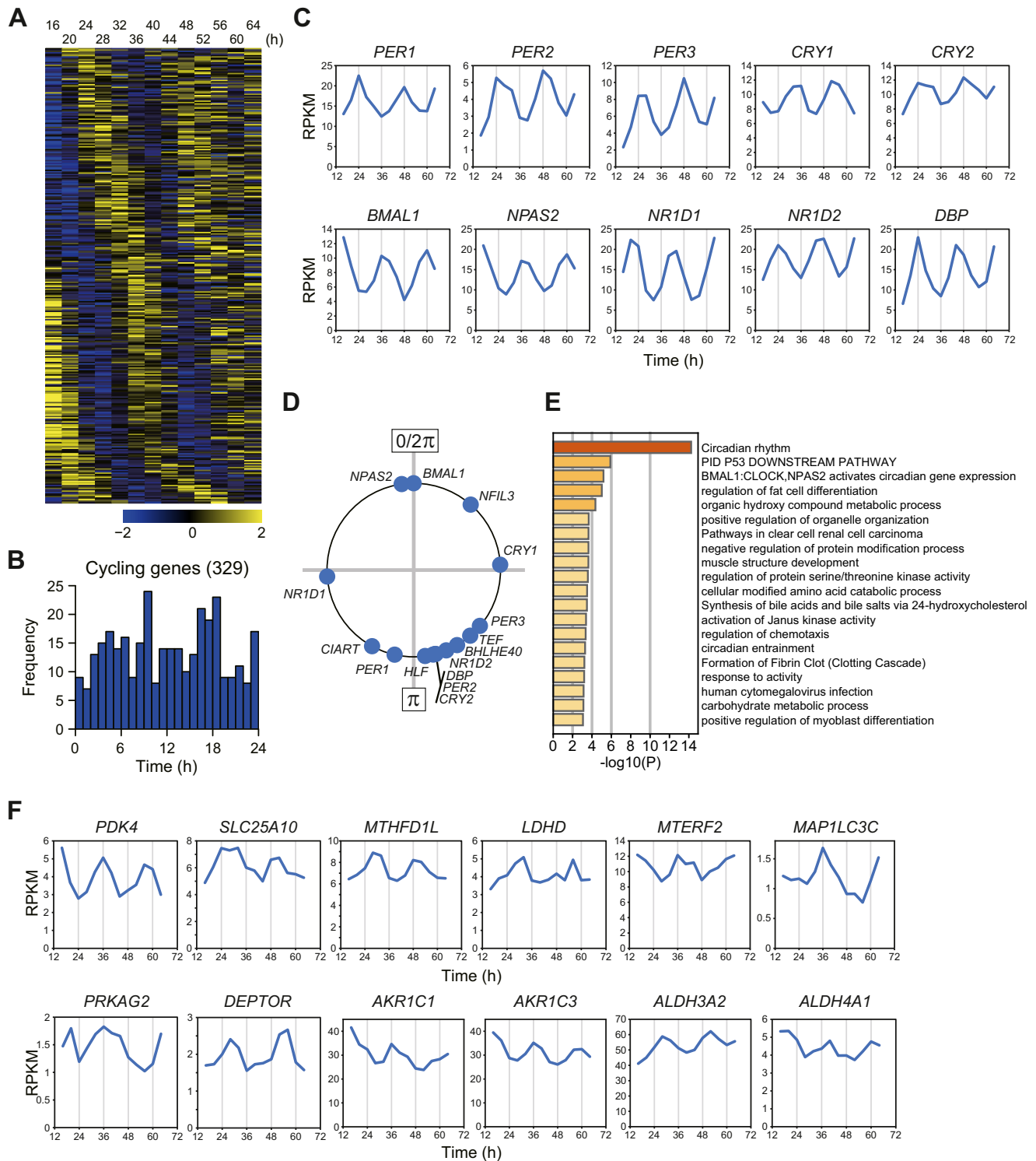


FIGURE 3. Comprehensive analysis of global circadian gene expression in chCECs. **(A)** Heatmap image of the cycling genes. Each gene is represented as a horizontal line ordered vertically by phase as determined by MetaCycle. The indicated time (h) means the time after dexamethasone treatment. **(B)** Phase distribution of the cycling genes. **(C)** Circadian expression of clock and clock-related genes in the chCECs. **(D)** Phase distribution of the clock and clock-related genes. Peak phase in radian was plotted in a circadian cycle. Peak phase of *BMAL1* expression was set to $0/2\pi$. **(E)** The top 20 enriched terms of functional enrichment analysis of 329 cycling genes obtained by Metascape. **(F)** mRNA expression rhythms of the cycling genes involved in glycolysis, mitochondrial function, and energy homeostasis.

and barrier function (*COL8A1*, *COL8A2*, *COL1A2*, and *COL12A1*), mitochondrial function (*ATP5F1B* and a number of mitochondrially encoded genes), and glycolysis (*SLC2A1*,

ENO1, and *ALDOA*) (Fig. 4A). The genes *PTGDS* and *ALCAM* (*CD166*) are also reportedly highly expressed in HCECs.^{41,42,44,45} Our gene ontology analysis rendered a

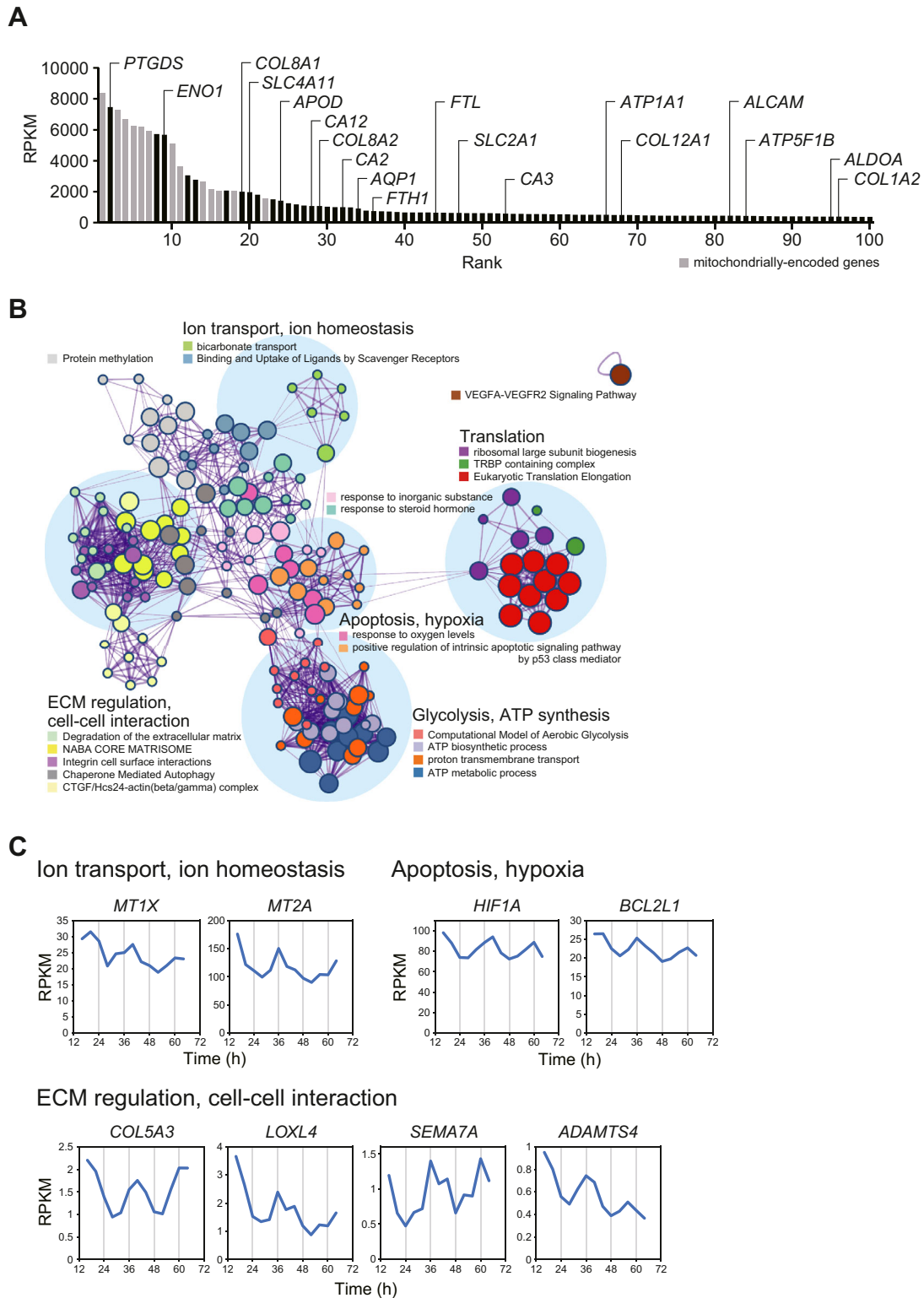


FIGURE 4. Circadian expression of genes involved in clusters of corneal endothelial function. **(A)** The top 100 highly expressed genes in the cHCECs. The average expression levels of 13 time-course samples were plotted. **(B)** The network view of the functional enrichment terms of 100 highly expressed genes obtained by Metascape analysis. **(C)** mRNA expression rhythms of the cycling genes involved in the indicated functions. The indicated time (h) means the time after dexamethasone treatment.

network plot of highly expressed genes in the cHCECs (Fig. 4B). Enriched terms likely represent important physiology and functions in HCECs, including translation, bicar-

bonate transport, ECM regulation, and response to oxygen level, as well as glycolysis and adenosine triphosphate biosynthesis.

Given the functional network, we identified a set of oscillating genes involved in each cluster of the enriched terms, including the genes *MT1X* and *MT2A* in the cluster of ion homeostasis, the genes *HIF1A* and *BCL2L1* in the cluster of hypoxic response and apoptosis, and the genes *COL5A3*, *LOXL4*, *SEMA7A*, and *ADAMTS4* in the cluster of ECM regulation (Fig. 4C). Collectively, these findings highlight the potential functional significance of the local circadian clock in corneal endothelium, although the physiological importance must be further evaluated.

DISCUSSION

To the best of our knowledge, the findings in this study are the first to identify the functional circadian clock in HCECs. Moreover, our further analysis of the global gene expression profiles demonstrated that a number of genes are expressed in a circadian manner in cHCECs. Given that the cornea is exposed to daily environmental changes, such as light and eyelid closure-induced hypoxia during sleep, maintaining a circadian homeostasis in corneal cells must surely be necessary. It was previously reported that the absence of the core clock gene *Bmal1* resulted in a loss of circadian regulations, an acceleration of aging, and a shortened life span in mice.⁴⁶ *Bmal1*-deficient mice develop ocular abnormalities such as a leukoplakic plaque on the cornea. Moreover, histological examinations have revealed corneal neovascularization, keratinization, and progressive inflammation.^{46,47} These observations suggest that circadian homeostasis is essential for maintaining a healthy cornea. Although the regulatory mechanism controlling circadian corneal physiology has yet to be fully elucidated, the highly robust circadian clock in cHCECs may represent the importance of the local circadian clock in corneal endothelium. Considering that circadian intraocular pressure rhythms primarily depend on dual pathways of glucocorticoid and the sympathetic nervous system, but not on the local ciliary clock,⁴⁸ further studies are needed to reveal the role of the local circadian clock in CECs.

Of note, although we focused on the circadian clock in CECs in this study, the circadian clock in other types of cells in cornea including immune cells, corneal neural cells, and stromal cells remains to be elucidated. Given that the circadian clock in corneal epithelial cells has been reported in mice previously,²² it should also be worth investigating the circadian clock in these specific types of cells in cornea.

One of the important roles of CECs is to maintain corneal transparency by pumping fluid from the stroma to the anterior chamber. To produce sufficient energy for active pumping, CECs are highly enriched with mitochondria to satisfy the continuous energy demand. The hypoxic condition during sleep leads to increased lactate production and is considered to increase energy demand for the pump function of corneal endothelium.⁴⁹ Given that the *PDK4* function acts as a switch from mitochondrial respiration to glycolysis, circadian regulation of *PDK4* expression may optimize energy production in accordance with circadian time of day. As it has been reported that *PDK4* expression is regulated by the circadian clock in murine peripheral tissues, including heart and skeletal muscle,^{50,51} circadian clock-dependent *PDK4* expression may represent a universal basis for circadian homeostasis of glucose and fatty acid utilization for energy production across tissues. Circadian expression of the gene *HIF1A* also highlights the fluctuation of glycolytic processes and oxygen metabolism in

HCECs. Accumulating evidence suggests that the circadian control of oxygen consumption and glycolysis is mediated via *HIF1 α* .^{52,53} Circadian expression of *PDK4* and *HIF1A* may serve as a system that predicts circadian time-dependent hypoxic conditions and energy demand, thus optimizing the energy production in HCECs. If the circadian clock has a role in energy production required for the maintenance of water flux, malfunction of circadian regulation could aggravate morning edema, which is often observed in bullous keratopathy. A previous study has shown that expression levels of genes involved in several pathways including glycolysis, responses to hypoxia, and oxidation-reduction processes are altered in the CECs of patients with bullous keratopathy.⁵⁴ Therefore, proper regulation of gene expression in these pathways would be related to normal corneal endothelial function, although further study is needed to evaluate the relevance of circadian regulation.

SLC25A10 is a mitochondrial carrier protein that transports the dicarboxylate substrates, thus regulating NADH synthesis and redox homeostasis to protect cells against oxidative stress.⁵⁵ Intriguingly, the findings in a previous study demonstrated that *CLOCK* can bind to and acetylate *SLC25A10* and regulate its function.⁵⁶ Circadian expression of *SLC25A10* has also been shown in the mouse liver. Thus, it is possible that *SLC25A10* also mediates circadian regulation of mitochondrial function in CECs. Reportedly, another mitochondrial gene, methylenetetrahydrofolate dehydrogenase 1-like (*MTHFD1L*), shows circadian expression in the mouse liver that is transcriptionally regulated by *CLOCK/BMAL1* via its E-box sequence.⁵⁷ Moreover, other genes implicated in the regulation of mitochondrial function and energy homeostasis, such as lactate dehydrogenase D (*LDHD*),⁵⁸ mitochondrial transcription termination factor 2 (*MTERF2*),⁵⁹ mitophagy regulator *MAL3C*,⁶⁰ a non-catalytic subunit of AMP-activated protein kinase (*PRKAG2*),⁶¹ and an inhibitory regulator of mTOR complex 1 (*DEPTOR*)⁶² also exhibit clear circadian mRNA expression rhythms. Considering that recent studies have revealed circadian regulation of mitochondrial morphology and generation, as well as respiratory function,⁶³ it may be important for metabolically active and mitochondria rich HCECs to coordinate energy balance and mitochondrial respiration with diurnal changes in environment.

Another important aspect of high mitochondrial activity is the enhanced production of reactive oxygen species (ROS). Oxidative stress has been implicated in the pathogenesis of corneal endothelial disorders, including FECD.^{64,65} Thus, it would be advantageous to upregulate antioxidative mechanisms against ROS, especially in the active phase of mitochondrial respiration. Circadian expression of antioxidant factors including metallothionein genes *MT1X* and *MT2A*, aldo/keto reductase genes *AKR1C1* and *AKR1C3*, and aldehyde dehydrogenase genes, such as *ALDH3A2* and *ALDH4A1*, may contribute to the prediction and counteraction of the daily raise of ROS produced by mitochondrial activity.^{66–69} In addition to those factors, anti-apoptotic *BCL2L1*, which reportedly shows circadian expression in various tissues, may participate in the defense system against oxidative stress.⁷⁰ In our analysis, the findings also identified genes involved in ECM regulation and cell-to-cell interaction, such as *SEMA7A*, *LOXL4*, *COL5A3*, and *ADAMTS4*. Reportedly, *SEMA7A* is expressed in the corneas of mice and links corneal nerve regeneration and inflammatory processes.⁷¹ Also, *LOXL4* is slightly decreased in keratoconus corneas⁷² and is essential to the wound-healing mechanism in human

corneal epithelial cells.⁷³ However, the relevance of those genes to the function of HCECs remains unclear. Further evaluation of circadian gene expression rhythms identified in this study is necessary to establish the physiological significance of the circadian clock in HCECs.

In this study, we used CD44^{-/-dull} mature differentiated cHCECs without CST, which mimic the characteristics of *in vivo* healthy-tissue HCECs and thus would be useful for evaluating the physiological relevance of the circadian clock in HCECs. To further elucidate the function of healthy CECs, a similar further study involving cHCECs with CST, which share the characteristics of damaged HCECs observed in corneal diseases such as FECD, may be required.⁷⁴ It is also important to investigate inter-individual differences in circadian gene expression using corneas from multiple donors in a future study. The identification of a robust and entrainable circadian clock in cHCECs suggests potential molecular links between the circadian clock and CEC function. Further analyses should be conducted to clarify circadian regulation in physiological processes including glycolysis and mitochondrial functions in HCECs. As our cHCECs should have kept the *in vivo* characteristics of CECs, this study could shed new light on the regulation of corneal endothelial function and pave the way for further understanding of human corneal physiology.

Acknowledgments

The authors thank Asako Uehara, Munetoyo Toda, Nao Hiramoto, Atsushi Mukai, and Suzune Nagao for their technical support and John Bush for editing the manuscript. This work was supported in part by Grants-in-Aid for Scientific Research from the Japan Society for the Promotion of Science (18K06338 to YT; 18H02600 and 21H02664 to KY), and by a grant from the Japan Science and Technology Agency JST-Mirai Program (19216520 to KY).

Disclosure: **H. Nakai**, None; **Y. Tsuchiya**, None; **N. Koike**, None; **T. Asano**, None; **M. Ueno**, None; **Y. Umemura**, None; **Y. Sasawaki**, None; **R. Ono**, None; **J. Hamuro**, None; **C. Sotozono**, None; **K. Yagita**, None

References

- Reppert SM, Weaver DR. Coordination of circadian timing in mammals. *Nature*. 2002;418(6901):935–941.
- Balsalobre A, Damiola F, Schibler U. A serum shock induces circadian gene expression in mammalian tissue culture cells. *Cell*. 1998;93(6):929–937.
- Yagita K, Tamanini F, van Der Horst GT, Okamura H. Molecular mechanisms of the biological clock in cultured fibroblasts. *Science*. 2001;292(5515):278–281.
- Yamazaki S, Numano R, Abe M, et al. Resetting central and peripheral circadian oscillators in transgenic rats. *Science*. 2000;288(5466):682–685.
- Bass J, Lazar MA. Circadian time signatures of fitness and disease. *Science*. 2016;354(6315):994–999.
- McMahon DG, Michael Iuvone P, Tosini G. Circadian organization of the mammalian retina: from gene regulation to physiology and diseases. *Prog Retin Eye Res*. 2014;39:58–76.
- Takahashi JS. Transcriptional architecture of the mammalian circadian clock. *Nat Rev Genet*. 2017;18(3):164–179.
- Yoo S-H, Yamazaki S, Lowrey PL, et al. PERIOD2::LUCIFERASE real-time reporting of circadian dynamics reveals persistent circadian oscillations in mouse peripheral tissues. *Proc Natl Acad Sci USA*. 2004;101(15):5339–5346.
- Preitner N, Damiola F, Molina , et al. The orphan nuclear receptor REV-ERB α controls circadian transcription within the positive limb of the mammalian circadian oscillator. *Cell*. 2002;110(2):251–260.
- Cho H, Zhao X, Hatori M, et al. Regulation of circadian behaviour and metabolism by REV-ERB- α and REV-ERB- β . *Nature*. 2012;485(7396):123–127.
- Nickla DL, Wildsoet C, Wallman J. Visual influences on diurnal rhythms in ocular length and choroidal thickness in chick eyes. *Exp Eye Res*. 1998;66(2):163–181.
- Read SA, Collins MJ, Iskander DR. Diurnal variation of axial length, intraocular pressure, and anterior eye biometrics. *Invest Ophthalmol Vis Sci*. 2008;49(7):2911–2918.
- Kikkawa Y. Diurnal variation in corneal thickness. *Exp Eye Res*. 1973;15(1):1–9.
- Kiely PM, Carney LG, Smith G. Diurnal variations of corneal topography and thickness. *Am J Optom Physiol Opt*. 1982;59(12):976–982.
- Harper CL, Boulton ME, Bennett D, et al. Diurnal variations in human corneal thickness. *Br J Ophthalmol*. 1996;80(12):1068–1072.
- du Toit R, Vega JA, Fonn D, Simpson T. Diurnal variation of corneal sensitivity and thickness. *Cornea*. 2003;22(3):205–209.
- Read SA, Collins MJ. Diurnal variation of corneal shape and thickness. *Optom Vis Sci*. 2009;86(3):170–180.
- Fritz M, Grewing V, Maier P, et al. Diurnal variation in corneal edema in Fuchs endothelial corneal dystrophy. *Am J Ophthalmol*. 2019;207:351–355.
- Fatt I, Bieber MT. The steady-state distribution of oxygen and carbon dioxide in the *in vivo* cornea. I. The open eye in air and the closed eye. *Exp Eye Res*. 1968;7(1):103–112.
- Efron N, Carney LG. Oxygen levels beneath the closed eyelid. *Invest Ophthalmol Vis Sci*. 1979;18(1):93–95.
- Benjamin WJ, Hill RM. Closed-lid factors influencing human corneal oxygen demand. *Acta Ophthalmol*. 1986;64(6):644–648.
- Baba K, Davidson AJ, Tosini G. Melatonin entrains PER2::LUC bioluminescence circadian rhythm in the mouse cornea. *Invest Ophthalmol Vis Sci*. 2015;56(8):4753–4758.
- Doughty MJ. Morphometric analysis of the surface cells of rabbit corneal epithelium by scanning electron microscopy. *Am J Anat*. 1990;189(4):316–328.
- Kinoshita S, Koizumi N, Ueno M, et al. Injection of cultured cells with a ROCK inhibitor for bullous keratopathy. *N Engl J Med*. 2018;378(11):995–1003.
- Hamuro J, Toda M, Asada K, et al. Cell homogeneity indispensable for regenerative medicine by cultured human corneal endothelial cells. *Invest Ophthalmol Vis Sci*. 2016;57(11):4749–4761.
- Hamuro J, Ueno M, Asada K, et al. Metabolic plasticity in cell state homeostasis and differentiation of cultured human corneal endothelial cells. *Invest Ophthalmol Vis Sci*. 2016;57(10):4452–4463.
- Numa K, Ueno M, Fujita T, et al. Mitochondria as a platform for dictating the cell fate of cultured human corneal endothelial cells. *Invest Ophthalmol Vis Sci*. 2020;61(14):10.
- Okumura N, Koizumi N, Ueno M, et al. ROCK inhibitor converts corneal endothelial cells into a phenotype capable of regenerating *in vivo* endothelial tissue. *Am J Pathol*. 2012;181(1):268–277.
- Hamuro J, Deguchi H, Fujita T, et al. Polarized expression of ion channels and solute carrier family transporters on heterogeneous cultured human corneal endothelial cells. *Invest Ophthalmol Vis Sci*. 2020;61(5):47.
- Yagita K, Horie K, Koinuma S, et al. Development of the circadian oscillator during differentiation of mouse embryonic stem cells *in vitro*. *Proc Natl Acad Sci USA*. 2010;107(8):3846–3851.

31. Bolger AM, Lohse M, Usadel B. Trimmomatic: a flexible trimmer for Illumina sequence data. *Bioinformatics*. 2014;30(15):2114–2120.
32. Dobin A, Davis CA, Schlesinger F, et al. STAR: ultrafast universal RNA-seq aligner. *Bioinformatics*. 2013;29(1):15–21.
33. Li H, Handsaker B, Wysoker A, et al. The sequence alignment/map format and samtools. *Bioinformatics*. 2009;25(16):2078–2079.
34. Heinz S, Benner C, Spann N, et al. Simple combinations of lineage-determining transcription factors prime cis-regulatory elements required for macrophage and B cell identities. *Mol Cell*. 2010;38(4):576–589.
35. Koike N, Yoo SH, Huang HC, et al. Transcriptional architecture and chromatin landscape of the core circadian clock in mammals. *Science*. 2012;338(6105):349–354.
36. Wu G, Anafi RC, Hughes ME, Kornacker K, Hogenesch JB. MetaCycle: an integrated R package to evaluate periodicity in large scale data. *Bioinformatics*. 2016;32(21):3351–3353.
37. Zhou Y, Zhou B, Pache L, et al. Metascape provides a biologist-oriented resource for the analysis of systems-level datasets. *Nat Commun*. 2019;10(1):1523.
38. Frausto RF, Le DJ, Aldave AJ. Transcriptomic analysis of cultured corneal endothelial cells as a validation for their use in cell replacement therapy. *Cell Transplant*. 2016;25(6):1159–1176.
39. Chow S, Ruskey F. Towards a general solution to drawing area-proportional Euler diagrams. *Electronic Notes Theor Comput Sci*. 2005;134:3–18.
40. Ueno M, Toda M, Numa K, et al. Superiority of mature differentiated cultured human corneal endothelial cell injection therapy for corneal endothelial failure. *Am J Ophthalmol*. 2022;237:267–277.
41. Sakai R, Kinouchi T, Kawamoto S, et al. Construction of human corneal endothelial cDNA library and identification of novel active genes. *Invest Ophthalmol Vis Sci*. 2002;43(6):1749–1756.
42. Gottsch JD, Seitzman GD, Margulies EH, et al. Gene expression in donor corneal endothelium. *Arch Ophthalmol*. 2003;121(2):252–258.
43. Frausto RF, Wang C, Aldave AJ. Transcriptome analysis of the human corneal endothelium. *Invest Ophthalmol Vis Sci*. 2014;55(12):7821–7830.
44. Tokuda Y, Okumura N, Komori Y, et al. Transcriptome dataset of human corneal endothelium based on ribosomal RNA-depleted RNA-Seq data. *Sci Data*. 2020;7(1):407.
45. Ding V, Chin A, Peh G, Mehta JS, Choo A. Generation of novel monoclonal antibodies for the enrichment and characterization of human corneal endothelial cells (hCENC) necessary for the treatment of corneal endothelial blindness. *Mabs*. 2014;6(6):1439–1452.
46. Kondratov RV, Kondratova AA, Gorbacheva VY, Vykhovanets OV, Antoch MP. Early aging and age-related pathologies in mice deficient in BMAL1, the core component of the circadian clock. *Genes Dev*. 2006;20(14):1868–1873.
47. Yang G, Chen L, Grant GR, et al. Timing of expression of the core clock gene Bmal1 influences its effects on aging and survival. *Sci Transl Med*. 2016;8(324):324ra16.
48. Ikegami K, Shigeyoshi Y, Masubuchi S. Circadian regulation of IOP rhythm by dual pathways of glucocorticoids and the sympathetic nervous system. *Invest Ophthalmol Vis Sci*. 2020;61(3):26.
49. Leung BK, Bonanno JA, Radke CJ. Oxygen-deficient metabolism and corneal edema. *Prog Retin Eye Res*. 2011;30(6):471–492.
50. Stavinoha MA, Rayspellicy JW, Hart-Sailors ML, Mersmann HJ, Bray MS, Young ME. Diurnal variations in the responsiveness of cardiac and skeletal muscle to fatty acids. *Am J Physiol Endocrinol Metab*. 2004;287(5):E878–E887.
51. Durgan DJ, Hotze MA, Tomlin TM, et al. The intrinsic circadian clock within the cardiomyocyte. *Am J Physiol Heart Circ Physiol*. 2005;289(4):H1530–H1541.
52. Peek CB, Levine DC, Cedernaes J, et al. Circadian clock interaction with HIF1 α mediates oxygenic metabolism and anaerobic glycolysis in skeletal muscle. *Cell Metab*. 2017;25(1):86–92.
53. Wu Y, Tang D, Liu N, et al. Reciprocal regulation between the circadian clock and hypoxia signaling at the genome level in mammals. *Cell Metab*. 2017;25(1):73–85.
54. Yamaguchi T, Higa K, Yagi-Yaguchi Y, et al. Pathological processes in aqueous humor due to iris atrophy predispose to early corneal graft failure in humans and mice. *Sci Adv*. 2020;6(20):eaaz5195.
55. Rochette L, Meloux A, Zeller M, Malka G, Cottin Y, Vergely C. Mitochondrial SLC25 carriers: novel targets for cancer therapy. *Molecules*. 2020;25(10):2417.
56. Cai T, Hua B, Luo D, et al. The circadian protein CLOCK regulates cell metabolism via the mitochondrial carrier SLC25A10. *Biochim Biophys Acta Mol Cell Res*. 2019;1866(8):1310–1321.
57. Masri S, Rigor P, Cervantes M, et al. Partitioning circadian transcription by SIRT6 leads to segregated control of cellular metabolism. *Cell*. 2014;158(3):659–672.
58. Drabkin M, Yogev Y, Zeller L, et al. Hyperuricemia and gout caused by missense mutation in D-lactate dehydrogenase. *J Clin Invest*. 2019;129(12):5163–5168.
59. Linder T, Park CB, Asin-Cayuela J, et al. A family of putative transcription termination factors shared amongst metazoans and plants. *Curr Genet*. 2005;48(4):265–269.
60. Le Guerroué F, Eck F, Jung J, et al. Autophagosomal content profiling reveals an LC3C-dependent piecemeal mitophagy pathway. *Mol Cell*. 2017;68(4):786–796.e6.
61. Herzig S, Shaw RJ. AMPK: guardian of metabolism and mitochondrial homeostasis. *Nat Rev Mol Cell Biol*. 2018;19(2):121–135.
62. Saxton RA, Sabatini DM. mTOR signaling in growth, metabolism, and disease. *Cell*. 2017;168(6):960–976.
63. de Goede P, Wefers J, Brombacher EC, Schrauwen P, Kalsbeek A. Circadian rhythms in mitochondrial respiration. *J Mol Endocrinol*. 2018;60(3):R115–R130.
64. Jurkunas UV, Bitar MS, Funaki T, Azizi B. Evidence of oxidative stress in the pathogenesis of Fuchs endothelial corneal dystrophy. *Am J Pathol*. 2010;177(5):2278–2289.
65. Vallabh NA, Romano V, Willoughby CE. Mitochondrial dysfunction and oxidative stress in corneal disease. *Mitochondrion*. 2017;36:103–113.
66. Ruttkay-Nedecky B, Nejdil L, Gumulec J, et al. The role of metallothionein in oxidative stress. *Int J Mol Sci*. 2013;14(3):6044–6066.
67. Burczynski ME, Sridhar GR, Palackal NT, Penning TM. The reactive oxygen species- and Michael acceptor-inducible human aldo-keto reductase AKR1C1 reduces the α,β -unsaturated aldehyde 4-hydroxy-2-nonenal to 1,4-dihydroxy-2-nonenone. *J Biol Chem*. 2001;276(4):2890–2897.
68. Demozay D, Rocchi S, Mas JC, et al. Fatty aldehyde dehydrogenase: potential role in oxidative stress protection and regulation of its gene expression by insulin. *J Biol Chem*. 2004;279(8):6261–6270.
69. Yoon KA, Nakamura Y, Arakawa H. Identification of ALDH4 as a p53-inducible gene and its protective role in cellular stresses. *J Hum Genet*. 2004;49(3):134–140.
70. Soták M, Sumová A, Pácha J. Cross-talk between the circadian clock and the cell cycle in cancer. *Ann Med*. 2014;46(4):221–232.

71. Namavari A, Chaudhary S, Ozturk O, et al. Semaphorin 7a links nerve regeneration and inflammation in the cornea. *Invest Ophthalmol Vis Sci.* 2012;53(8):4575–4585.
72. Dudakova L, Sasaki T, Liskova P, Palos M, Jirsova K. The presence of lysyl oxidase-like enzymes in human control and keratoconic corneas. *Histol Histopathol.* 2016;31(1):63–71.
73. Comptour A, Rouzaire M, Belville C, et al. Lysyl oxidase-like 4 involvement in retinoic acid epithelial wound healing. *Sci Rep.* 2016;6:32688.
74. Ueno M, Asada K, Toda M, et al. MicroRNA profiles qualify phenotypic features of cultured human corneal endothelial cells. *Invest Ophthalmol Vis Sci.* 2016;57(10):5509–5515.

SUPPLEMENTARY MATERIAL

SUPPLEMENTARY VIDEO. The *Bmal1:luc* bioluminescence rhythms in hCECs.